Structure and dynamics of ferroelectric pyridinium periodate

2001 J. Phys.: Condens. Matter 13 11053

(http://iopscience.iop.org/0953-8984/13/48/329)

INSTITUTE OF PHYSICS PUBLISHING JOURNAL OF PHYSICS: CONDENSED MATTER

J. Phys.: Condens. Matter **13** (2001) 11053–11065 PII: S0953-8984(01)28156-9

Structure and dynamics of ferroelectric pyridinium periodate

H Małuszyńska[1], P Czarnecki[1], S Lewicki[1], J Wąsicki[1] and M Gdaniec[2]

[1] Faculty of Physics, A. Mickiewicz University, Umultowska 85, 61-614 Poznań, Poland
[2] Faculty of Chemistry, A Mickiewicz University, Grunwaldzka 6, 60-780 Poznań, Poland

Received 23 August 2001, in final form 25 October 2001
Published 16 November 2001
Online at stacks.iop.org/JPhysCM/13/11053

Abstract

The crystal and molecular structure of a new ferroelectric from the pyridinium salt group $[C_5H_5NH]^+IO_4^-$ was determined by the x-ray diffraction method at 350, 300 and 100 K. The high temperature and intermediate phases are orthorhombic, while the low temperature phase is monoclinic, with the following sequences of space groups and continuous phase transitions: $Cmcm \xrightarrow{321\ K} Cmc2_1 \xrightarrow{210\ K} C2$. The two orthorhombic phases are isostructural with $PyReO_4$, where the pyridinium cation is disordered and the periodate anion is ordered. The low temperature phase is well ordered. The intermediate and low temperature phases are ferroelectric. Measurements of spin-lattice relaxation time and complex permittivity have been performed for polycrystalline and monocrystalline samples as a function of pressure and temperature. The potential shape and heights of the energy barriers for cation reorientations in ferroelectric phases have been proposed. The complex permittivity measurements indicate the order–disorder character of the ferroelectric phase transition and continuous slowing of the cation dynamics with decreasing temperature.

(Some figures in this article are in colour only in the electronic version)

1. Introduction

Pyridinium periodate ($PyIO_4$) is the fourth member of the recently discovered family of ferroelectric crystals [1]. The structure of $PyIO_4$ was determined only at the room temperature phase [2]. The common features characterizing the members of the family of ferroelectric pyridinium salts are the occurrence at least two solid–solid phase transitions [3–7] and the tetrahedral structure of the anion (BF_4^-, ClO_4^-, ReO_4^-, IO_4^-). With regard to the symmetry of the prototype (high temperature) phase, this family can be divided into two groups. The first includes $PyBF_4$ and $PyClO_4$, which in the high temperature phases are trigonal [4, 7], while the second group comprises $PyReO_4$ and $PyIO_4$, which in the intermediate phases are

orthorhombic [2, 7]. The low and high temperature phases have been determined only for $PyReO_4$ but not for $PyIO_4$.

In the pyridinium salts studied so far by NMR, dielectric and neutron spectroscopies [3–6, 8–14], the dynamics of the cation was similar. In all phases the pyridinium cation was found to reorient about the pseudo-hexagonal axis perpendicular to the plane of the ring; in the low temperature and intermediate phases the reorientation occurs over inequivalent potential energy barriers, while in the high temperature phase it occurs over equivalent barriers. The asymmetry parameter (the energy difference between the potential energy minima) depends on temperature and decreases with its increase. NMR results have suggested that the tetrahedral anions also undergo reorientation and the structural study has not excluded a small deviation from the tetrahedral symmetry [8]. Therefore it can be expected that not only the pyridinium cation but also the anions will show a non-zero dipole moment. Therefore the ferroelectric properties of the pyridinium salts can be related to the dynamics of the cationic and anionic sublattices. Brillouin spectra clearly revealed a small quasielastic component at room temperature, which is, in fact, coupled to longitudinal acoustic modes along all directions [15], which means the complex nature of the ion interactions in pyridinium salts.

The polycrystalline samples of $PyIO_4$ have been studied by the dielectric method, NMR, DTA and Raman spectroscopy [1,16,17] and a hysteresis loop was observed for these samples in the intermediate phase. Recently, monocrystalline samples have also been studied by dielectric spectroscopy and birefringence methods [17]. These samples revealed hysteresis loops in the intermediate and low temperature phases.

The aim of this paper is to present the single-crystal x-ray structural results of high and low temperature phases and the dynamics study of $PyIO_4$ by pressure NMR, dielectric spectroscopy for polycrystalline and monocrystalline samples, respectively.

2. Experiments

X-ray data were collected on a KM-4 diffractometer with KUMA-CCD camera, using Mo Kα radiation and a graphite monochromator and ω–2Θ scan technique. The cycles of cooling and heating were carried out at a rate of 120 K h^{-1} using Oxford Cryosystem. The Lorentz polarization and semi-empirical absorption corrections were applied. A summary of crystal data and structure refinement details are given in table 1. Atomic coordinates and equivalent temperature factors for $PyIO_4$ at 350, 300 and 100 K are presented in table 2. Bond lengths [Å] and angles [°] are presented in table 3.

The proton spin-lattice relaxation times T_1 for a polycrystalline sample were measured under hydrostatic pressure using a set-up including a pulse NMR spectrometer working at 25 MHz, an UNIPRESS U-11 helium gas compressor and a beryllium–copper high pressure cell [18].

Complex permittivity measurements were performed for a few frequencies from 1 kHz to 13 MHz using an impedance analyser HP-4192 A, from Hewlett-Packard. The measurements were performed using a sample of size $2 \times 2 \times 1$ mm in the direction of the twofold polar axis of the orthorhombic system.

3. Results and discussion

3.1. X-ray results

Structures of the three phases were solved by the Patterson method (SHELXS-97 [19]) and refined anisotropically by the full-matrix least squares technique using SHELXL-97 [20]. The

Table 1. Crystal data and structure refinement for pyridinium periodate $[C_5H_5NH]^+[IO_4]^-$ at 350, 300 and 100 K.

Temperature	350 K	300 K	100 K
Formula weight (g)		271.01	
Wavelength (Å)		0.71073	
Crystal system	Orthorhombic	Orthorhombic	Monoclinic
Space group	$Cmcm$	$Cmc2_1$	$C2$
Unit cell dimension (Å)	8.422(2)	8.283(2)	8.245(2)
	7.367(1)	7.175(1)	7.122(1)
	12.789(3)	12.779(3)	12.780(3)
			$\beta = 90.00$
Volume (Å^3)	793.5(3)	759.5(3)	750.5(3)
Z	4	4	4
Density (calculated) Mg m^{-3}	2.269	2.370	2.399
Absorption coefficient	4.003	4.182	4.233
$F(000)$	512	512	512
Crystal size (mm)		$0.4 \times 0.4 \times 0.25$	
Theta range (deg)	$3.7 \div 29.9$	$3.8 \div 29.9$	$3.8 \div 29.4$
Reflections collected	2967	2799	4223
Unique, R(int)	559, 0.05	1007, 0.05	1731, 0.069
Refinement method		Full-matrix least squares on F^2	
Data/restraints/parameters	595/0/32	1007/1/57	1731/7/103
Goodness of fit on F^2	1.064	1.064	1.100
R indices $[I > 2\sigma(I)]$	$R_1 = 0.0638$	$R_1 = 0.0576$	$R_1 = 0.0565$
	$wR_2 = 0.2012$	$wR_2 = 0.1644$	$wR_2 = 0.1463$
R indices (all data)	$R_1 = 0.0716$	$R_1 = 0.0658$	$R_1 = 0.0569$
	$wR_2 = 0.2130$	$wR_2 = 0.1774$	$wR_2 = 0.1469$
Extinction coefficient	0.022(6)	0.018(3)	0.029(3)
Absolute structure parameter	—	0.6(3)	0.43(16)
Largest difference peak and hole (eÅ^{-3})	1.93, −1.07	2.57, −2.17	3.06, −5.94

hydrogen atom positions were calculated assuming C–H and N–H distances of 1.08 and 1.03 Å, respectively, and their parameters were refined isotropically as a riding model.

The high temperature and intermediate phases (I and II) at 350 and 300 K are isostructural with Py ReO_4 [8]. At 350 K, the space group is $Cmcm$, the pyridinium cation having symmetry $2/m$ is dynamically disordered. The N atom position is not distinguishable from the C atom. The IO_4 anion is well ordered.

In the intermediate phase (II) at 300 K the crystal structure loses the centre of symmetry and the space group becomes $Cmc2_1$. The pyridinium cation is disordered with the mirror m plane perpendicular to two C–C bonds and the N atom indistinguishable from the C atoms. The IO_4 anion is ordered, with the mirror plane passing through I, O(2) and O(3). At the end of the refinement a racemic twinning model was introduced, giving better convergence with the Flack [21] absolute structure x parameter of 0.6.

The low temperature phase (III) at 100 K is monoclinic, the space group is $C2$ with no significant changes in cell parameters, the monoclinic β angle included. The mirror m plane perpendicular to the x axis and the c plane perpendicular to the y axis disappear and the two-fold axis parallel to y becomes the only symmetry element, except for the c centring. Although there is a significant change in the crystal symmetry on cooling the molecular symmetry remains almost unchanged. Both ions are ordered, the periodate

Table 2. Atomic coordinates ($\times 10^4$) and equivalent isotropic displacement parameters ($\times 10^3$ Å^2) for $PyIO_4$ at (a) 350 K, (b) 300 K, (c) 100 K. U (eq) is defined as one-third of the trace of the orthogonalized U_{ij} tensor; o.f. is an occupancy factor.

	x/a	y/b	z/c	U(eq)	o.f.
(a) $T = 350$ K					
I(1)	0	6442(1)	2500	68(1)	0.25
O(1)	0	5130(30)	1352(9)	128(4)	0.50
O(2)	1696(9)	7786(18)	2500	113(3)	0.50
C(1)	1602(10)	0	5000	86(3)	0.50
C(2)	826(13)	982(12)	4294(9)	85(2)	1.0
H(1)	2884	0	5000	80	0.50
H(2)	1464	1790	3728	80	1.0
(b) $T = 300$ K					
I(1)	0	1467(1)	4998(10)	47(1)	0.50
O(1)	−1712(16)	2857(17)	5050(50)	87(4)	1.0
O(2)	0	−130(40)	6040(30)	78(10)	0.50
O(3)	0	400(60)	3790(20)	91(12)	0.50
C(1)	−820(40)	5900(40)	3160(20)	62(8)	1.0
C(2)	−1628(15)	4910(80)	2470(50)	62(5)	1.0
C(3)	−850(30)	3900(40)	1740(15)	55(6)	1.0
H(1)	−1455	6697	3750	80	1.0
H(2)	−2930	4982	2489	80	1.0
H(3)	−1532	3099	1181	80	1.0
(c) $T = 100$ K					
I(1)	0	1516(2)	5000	36(1)	0.50
O(1)	−1540(30)	3030(30)	5011(13)	89(1)	1.0
O(2)	−18(17)	30(30)	3899(13)	61(16)	1.0
I(2)	0	8399(1)	10000	6(1)	0.50
O(3)	−1784(12)	6990(20)	9986(12)	34(3)	1.0
O(4)	−18(17)	9630(30)	11190(12)	53(5)	1.0
N(1)	−800(20)	6070(20)	3249(11)	36(4)	1.0
C(2)	780(20)	6040(30)	3237(12)	28(3)	1.0
C(3)	1680(20)	4960(30)	2490(12)	31(4)	1.0
C(4)	854(17)	3950(20)	1792(12)	22(3)	1.0
C(5)	−855(16)	3950(20)	1787(1)	19(3)	1.0
C(6)	−1660(20)	4960(30)	2492(12)	30(4)	1.0
H(1)	−1403	6881	3786	40	1.0
H(2)	1442	6860	3814	40	1.0
H(3)	3005	4942	2502	40	1.0
H(4)	1508	3133	1208	40	1.0
H(5)	−1514	3118	1208	40	1.0
H(6)	−2983	4940	2502	40	1.0

atoms are located on the two-fold axis and occupy two special positions a and b (Wyckoff's letters). The two periodate atoms are related with pseudo-c plane perpendicular to the y axis. The pyridinium cation is well ordered with a pseudo-mirror plane perpendicular to the x axis.

The crystal structure in all three phases is almost identical. It consists of isolated tetrahedral IO_4 anions linked by weak X–H . . . O (X = C or N) bifurcated hydrogen bonds with pyridinium cations. The X–H . . . O values differ from 3.199–3.442 Å in phase I, 3.218–3.458 Å in phase II

Table 3. Bond lengths (a) and valency angles (deg) in $PyIO_4$ at (a) 350 K, (b) 300 K, (c) 100 K.

Bond	Length (Å)	Atoms	Angle (deg)
(a) $T = 350$ K			
I–O(1)	1.759(10)	O(1)–I–O(2)	108.3(4)
I–O(2)	1.738(9)	O(1)–I–O(1)[b]	113.1(13)
		O(2)–I–O(2)[a]	
C(1)–C(2)	1.329(12)	C(2)–C(1)–C(2)[c]	110.5(8)
C(2)–C(2)[d]	1.39(2)	C(1)–C(2)–C(2)[d]	121.1(11)
			119.4(5)
(b) T=300 K			
I–O(1)	1.735(11)	O(1)–I–O(2)	110.3(18)
I–O(2)	1.75(3)	O(1)–I–O(3)	107(2)
I–O(3)	1.72(3)	O(1)–I–O(1)[d]	109.6(9)
		O(2)–I–O(3)	112.8(15)
C(1)–C(2)	1.32(6)	C(2)–C(1)–C(1)[d]	120.5(15)
C(1)–C(1)[d]	1.36(6)	C(1)–C(2)–C(3)	120.7(13)
C(2)–C(3)	1.35(6)	C(2)–C(3)–C(3)[d]	118.7(17)
C(3)–C(3)[d]	1.40(5)		
(c) $T = 100$ K			
I(1)–O(1)	1.663(14)	O(1)–I(1)–O(2)	112.9(9)
I(1)–O(2)	1.760(12)	O(1)–I(1)–O(1)[e]	99.4(19)
I(2)–O(3)	1.782(12)	O(2)–I(1)–O(1)[e]	112.8(9)
I(2)–O(4)	1.754(13)	O(1)[e]–I(1)–O(2)[e]	112.9(9)
		O(2)–I(1)–O(2)[e]	106.3(16)
N(1)–C(2)	1.30(2)	O(3)–I(2)–O(4)	106.4(7)
N(1)–C(6)	1.44(2)	O(4)–I(2)–O(4)[f]	120.2(15)
		O(3)–I(2)–O(3)[f]	111.3(9)
C(2)–C(3)	1.43(3)	C(2)–N(1)–C(6)	118.7(16)
C(3)–C(4)	1.33(2)	N(1)–C(2)–C(3)	122.5(16)
C(4)–C(5)	1.409(18)	C(2)–C(3)–C(4)	117.9(16)
C(5)–C(6)	1.33(2)	C(3)–C(4)–C(5)	121.1(16)
		C(4)–C(5)–C(6)	119.4(15)
		N(1)–C(6)–C(5)	120.3(16)

[a] $-x, y, -z + 1/2$.
[b] $x, y, -z + 1/2$.
[c] $x, -y, -z + 1$.
[d] $-x, y, z$.
[e] $-x, y, -z + 1$.
[f] $-x, y, -z + 2$.

and in phase III is equal to 3.343 Å. Unit cell contents along the x axis at 350, 300 and 100 K are given in figures 1(a)–(c), respectively, and along the y axis in figures 2(a)–(c).

3.2. NMR results

The main aim of the study by nuclear magnetic relaxation as a function of temperature and pressure was to establish a model of reorientations of the pyridinium cation and determination of the activation parameters.

Measurements of the spin-lattice relaxation time T_1 were performed at temperatures from 154–322 K. The results are presented in figure 3. The vertical lines mark the phase transition

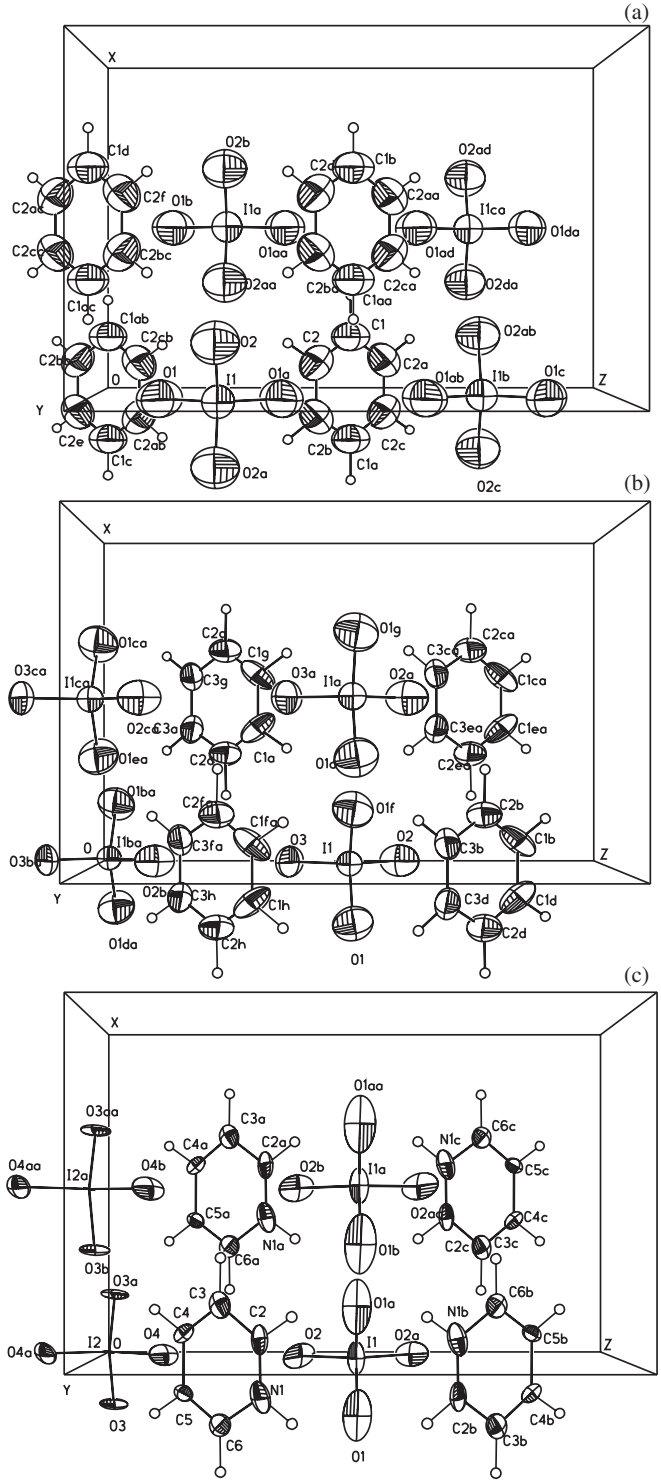

Figure 1. The packing arrangement in three phases at (a) 350 K, (b) 300 K and (c) 100 K in the *yz* plane.

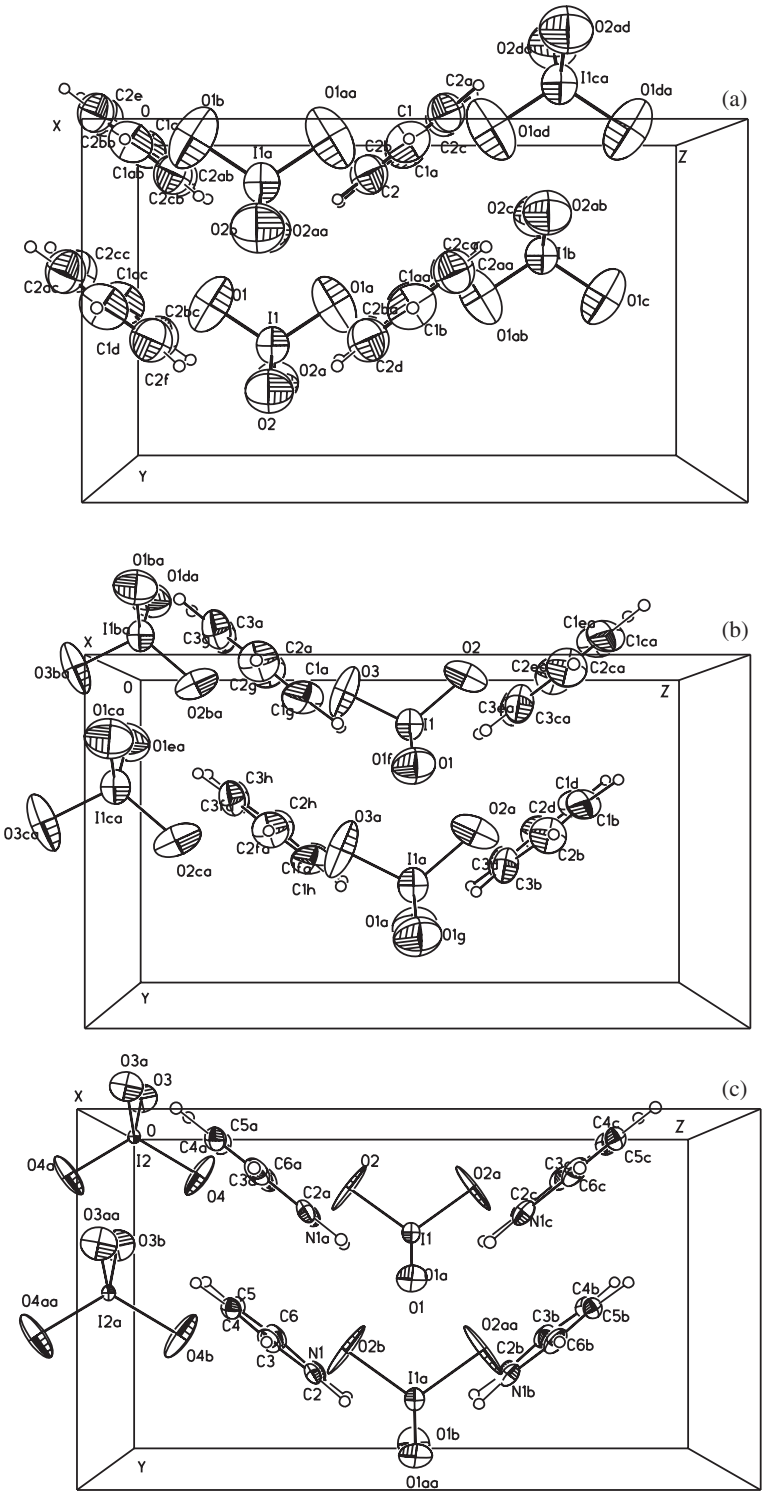

Figure 2. The packing arrangement in three phases at (a) 350 K, (b) 300 K and (c) 100 K in the xz plane.

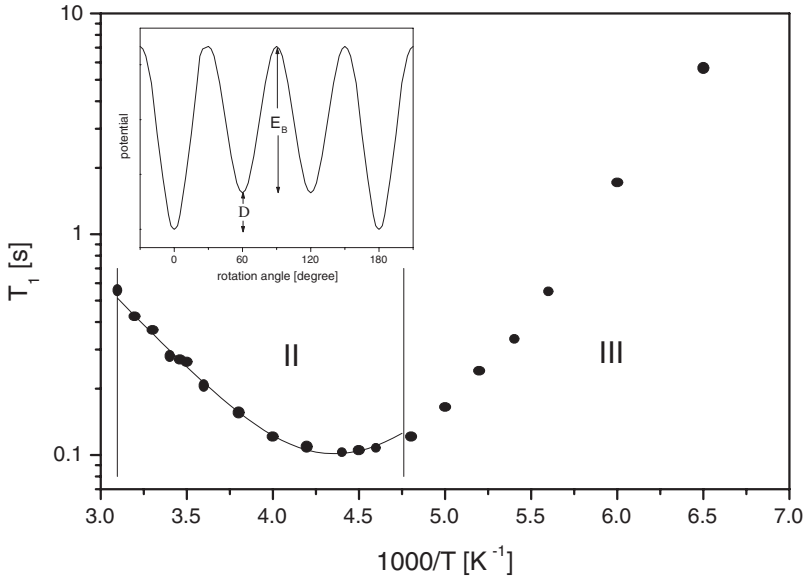

Figure 3. The dependence of T_1 on the inverse temperature. The shape of the potential for the model of reorientations over the inequivalent barriers is shown in the inset.

temperatures. The dependence of T_1 on the inverse temperature reveals a minimum of 102 ms at 227 K. The phase transition from phases II to III, taking place at 210 K, does not affect this dependence ($\ln T_1(1000/T)$) in a noticeable way. The results were interpreted assuming reorientational jumps of the pyridinium cation about the pseudo-hexagonal symmetry axis C_6' over the equivalent (i) and inequivalent (ii) potential barriers. The shape of the potential for the model of reorientations over the inequivalent barriers is shown in figure 3 (inset). It is described in terms of two parameters, the barrier height E_B and the parameter of asymmetry Δ, being the energy difference between the potential energy minima. The neighbouring minima are separated by 60°, while the barrier E_A is a sum of E_B and Δ. The influence of molecular reorientations over inequivalent potential barriers on the magnetic nuclear relaxation has been discussed in the literature [22,23]. The formulae describing the temperature dependence of the T_1 relaxation time for this model of reorientations have been derived in [10,24]. Of course, for $\Delta = 0$ we have the model of reorientations over equivalent barriers for which the T_1 behaviour is described by a well-known BPP formula [25].

From the best fit of the above formulae for T_1 to the experimental values we could find the activation parameters. The fitting procedure was performed for two temperature ranges:

(i) from 154–322 K, covering phases II and III,
(ii) from 210–322 K, covering phase II.

The results are given in table 4. In figure 3 the full curve marks the fitting results for phase II. Because in phase III there is no minimum of the T_1 relaxation time, it was only possible to estimate the activation energy for reorientation of the pyridinium cation as 20.7 kJ mole^{-1}.

As follows from analysis of the data in table 4:

(1) It is impossible to describe the temperature dependence of T_1 over the entire range of temperatures studied, covering phases II and III, with the help of the same set of activation parameters for the model of equivalent barriers because the standard deviation for this kind of fit exceeds 10%.

Table 4. The activation parameters for pyridinium periodate.

Temperature range	τ_0 (s)	E_B(kJ mol$^{-1)}$	Δ(kJ mol^{-1})	SD (%)
154–322 K	4×10^{-13}	17.6	—	11.9
Phases II, III	6.8×10^{-13}	16.9	4	5.8
210–322 K	1.1×10^{-12}	15.6	—	2.3
Phase II	8.7×10^{-13}	16.3	4.1	2.3

(2) For phase II the temperature dependence of T_1 can be described with the same accuracy for the model of equivalent and inequivalent barriers.

It is known that, for reorientation over equivalent potential barriers, the ratio of T_1 relaxation times at the minimum measured at different resonance frequencies is equal to the ratio of the resonance frequencies [25]. For the reorientation over the inequivalent potential barriers the ratio of T_1 relaxation times at the minimum is described by the expression [26]

$$T_1^{\min}(\omega_1)/T_1^{\min}(\omega_2) = (\omega_1/\omega_2)^{(1-\Delta/E_B)}. \tag{1}$$

As follows from the earlier results of T_1 measurements at 60 MHz, the minimum of this time, 200 ms, occurs at 250 K [4]. Therefore the ratio of $T_1^{\min}(60\ \text{MHz})/T_1^{\min}(25\ \text{MHz}) = 1.96$ and is lower than the frequency ratio equal to 2.4. Substituting the data from table 4 into equation (1) ($\Delta = 4.1$ kJ mol^{-1} and $E_B = 16.3$ kJ mol^{-1}) the ratio $T_1^{\min}(60\ \text{MHz})/T_1^{\min}(25\ \text{MHz}) = 1.93$, close to 1.96. Therefore, the reorientation of the pyridinium cation over the inequivalent potential barriers seems more probable.

Since the question of cation reorientation seems to be of great importance for the model of ferroelectricity in this crystal, the proposed model was verified by measurements of the effect of hydrostatic pressure on the relaxation time T_1 in phase II. These measurements were performed at pressures of 100, 200 and 300 MPa. With increasing pressure the minimum of the relaxation time is shifted towards higher temperatures and its value decreases. Figure 4 presents the pressure dependence of the temperature $T_{\min}$ and its value. According to our earlier work [24, 27] a decrease in the relaxation time T_1 with increasing pressure proves that the cation undergoes reorientations over inequivalent potential barriers. For the simplest case of two equivalent potential energy minima, knowing the pressure dependence temperature of T_1 we can find the ratio of the activation volume ΔV^* to the height of the barrier E_B from the formula [24]

$$\partial T_{\min}/\partial p = T_{\min}^0 \Delta V^*/E_B \tag{2}$$

where $T_{\min}^0$ is the temperature of the $T_{1\,\min}$ for normal pressure.

Putting $\partial T_{\min}/\partial p$ equal to 0.037 K MPa^{-1} (figure 4), and $T_{\min}^0$ of 227 K, the change in the activation volume was estimated as $\Delta V^*/E_B = 1.6 \times 10^{-4}$ MPa^{-1}. If E_B is taken as 16.3 kJ mol^{-1} (table 4) the activation volume in phase II is $\Delta V^* = 2.6$ cm^3 mol^{-1}.

On the basis of the pressure dependence of the T_1 relaxation time minimum the asymmetry parameter Δ can be obtained from the following formula [24]:

$$\partial \ln(T_1)_{\min}/\partial p = [\Delta/RT_{\min}^0(1 + \Delta V^* p/E_B)^2]\Delta V^*/E_B. \tag{3}$$

For $\partial \ln(T_1)_{\min}/\partial p = 3.8 \times 10^{-4}$ MPa^{-1} (figure 4), the asymmetry parameter was $\Delta = 4.9$ kJ mol^{-1}. Its value, obtained from the pressure dependence of T_1, is close to that estimated from the temperature dependence of T_1 under normal pressure.

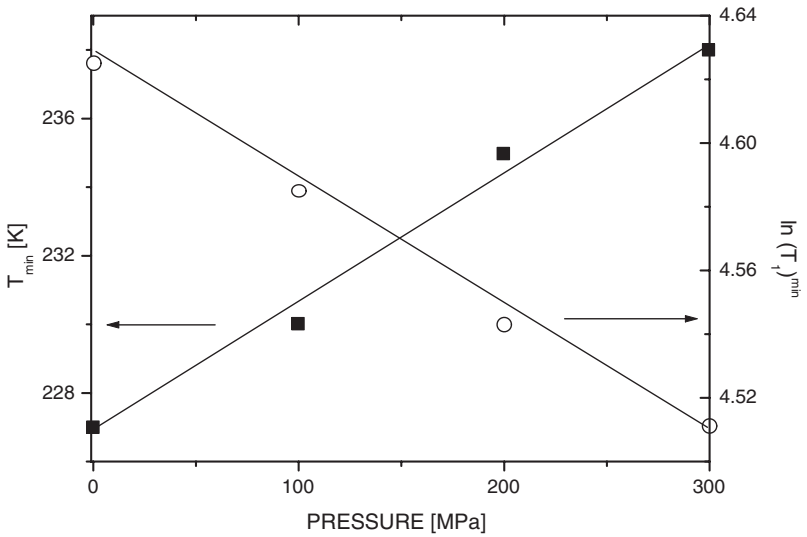

Figure 4. The pressure dependence of the temperature $T_{\min}$ and its value.

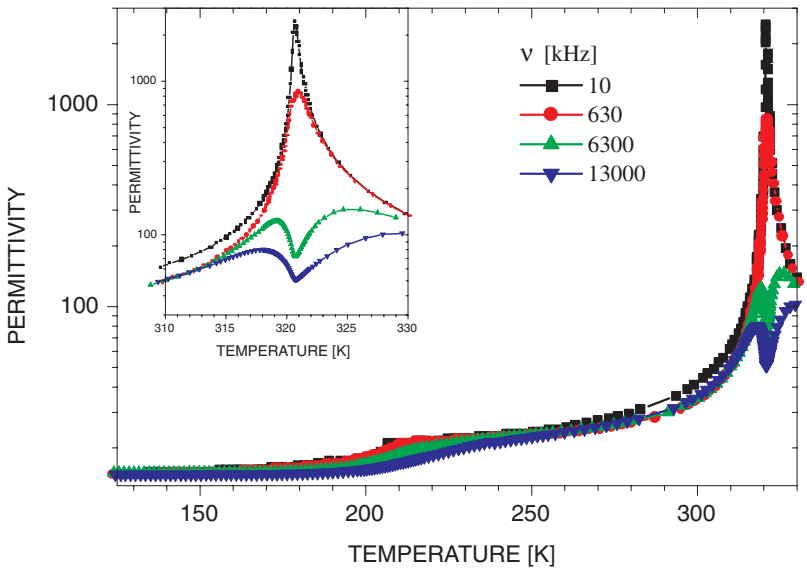

Figure 5. Permittivity dependence on temperature.

3.3. Dielectric measurements

Results of the temperature measurements of permittivity and loss tangent are shown in figures 5 and 6, respectively. Anomalies of permittivity appear at the temperatures of the ferroelectric ($T_{c1} = 321$ K) and non-ferroelectric ($T_{c2} = 210$ K) phase transitions. Apart from the anomalies related to the phase transitions, the temperature dependence of the loss tangent reveals maxima typical of dipolar relaxation processes in the material studied. The maxima appear in the three temperature ranges. In the low temperature range (below T_{c2}) there are small maxima, proving

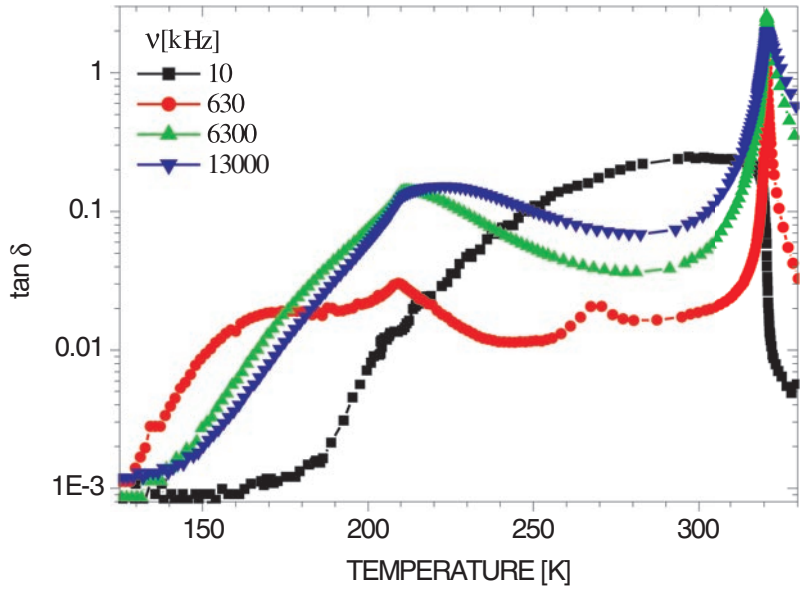

Figure 6. Loss tangent tan δ dependence on temperature.

the occurrence of reorientations even in the ordered phase. In the intermediate phase between T_{c2} and T_{c1}, there are two groups of maxima, which means the occurrence of two kinds of relaxation processes. One of them (a 10 kHz curve in figure 6) is related to the ferroelectric domain structure in the ferroelectric phase because the maxima of this group disappear after application of an external electric field. At temperatures close to the ferroelectric phase transition the so-called critical slowing down is observed, characterized by a sharp maximum of permittivity for low frequencies ($\varepsilon \approx 7000$) and minima for high frequencies (figure 5). The critical slowing down noted for the measuring electric field frequency of a few MHz means that $PyIO_4$ is an order–disorder type ferroelectric.

The main structural element of $PyIO_4$ is a flat pyridinium cation having a dipole moment. Its thermally activated reorientation is the origin of the observed dipolar relaxation. The relaxation time is usually described by the Arrhenius relation

$$\tau = \tau_0 \exp(\Delta H/RT) \tag{4}$$

where ΔH is the activation enthalpy of the relaxation process and τ_0 is the pre-exponential factor. When the condition $\omega\tau = 1$ is fulfilled, the temperature dependences of the imaginary permittivity and loss tangent will show a maximum. For each measuring frequency the maximum occurs at different temperature, so from the slope of $\ln\tau$ as a function of $1/T$ we can find the activation enthalpy ΔH and the pre-exponential factor τ_0. A more detailed interpretation of the dielectric results is difficult because the maxima of the loss tangent occur at temperatures close to that of the phase transition T_{c2} and on the shoulders caused by pre-transition effects.

The activation enthalpy determined in the low temperature phase is $\Delta H = 17 \pm 2$ kJ mol^{-1}, while in the intermediate phase $\Delta H = 16.5 \pm 2$ kJ mol^{-1}. The enthalpies of the reorientation processes in these two phases are similar, which means that the change in the dynamics of the pyridinium cations at the temperature of the continuous phase transition T_{c2} is small. The activation enthalpy values obtained by the dielectric method and NMR are similar for similar reorientations. The ferroelectric high temperature phase, in which the pyridinium

ions undergo reorientation about the pseudo-hexagonal symmetry axis, is strongly disordered. Although the phase transition at T_{c1} is of order–disorder type, the intermediate phase, between the temperatures T_{c1} and T_{c2} should also be classified as disordered because of the reorientations of the pyridinium cation detected by the dielectric method and NMR. The difference between the disordered paraelectric phase and partly ordered ferroelectric phase is due to the change of the pyridinium cation reorientations. In the paraelectric phase the reorientations take place between equivalent minima of potential energy, while in the ferroelectric phase one of the minima is deeper, so the time of residence of the cation at this minimum is longer. Although the difference in the cation dynamics is small, it is responsible for the symmetry breaking at T_{c1} , leading to a disappearance of one of the symmetry planes passing through the cation. This change results in the appearance of the ferroelectric polar phase $Cmc2_1$ and the origin of the permanent dipole moment is the partial ordering of the dipoles of the pyridinium cation. The ferroelectricity is a cooperative phenomenon, so the appearance of spontaneous polarization is due to the interaction of electric dipoles. We suppose that the tetrahedral IO_4anions also contribute to the appearance of ferroelectricity. Although the regular IO_4 tetrahedrons should not have dipole moments, however, in the ferroelectric phase a small dipole moment can appear as a result of the deformation of the tetrahedrons.

The ferroelectric phase transition is related to a change of the point group

$$mmm \overset{T=321\ \mathrm{K}}{\longrightarrow} mm2.$$

Such a change of symmetry means that there are two directions of spontaneous polarization along the two-fold axis of the orthorhombic system and that the transition is not ferroelastic. The crystal of $PyIO_4$ should be classified as an order–disorder ferroelectric.

The symmetry of the phase below T_{c2} is controversial. At the phase transition from $Cmc2_1$ to $C2$, the vector of spontaneous polarization must be rotated by 90° from the z axis of orthorombic $mm2$ to the y axis of monoclinic 2 symmetry, which contradicts the results of [17]. It is expected that more accurate structural measurements by neutron diffraction should resolve this question.

Although the structures of $PyIO_4$ and $PyReO_4$ [8] in the prototype and intermediate phases are identical, the low temperature phases are quite different. The low temperature phase transition at T_2 in $PyIO_4$ is continuous and discontinuous in $PyReO_4$. The low temperature structure of $PyIO_4$ is polar, and of $PyReO_4$ it is centrosymmetric. Similar differences in structure and physical properties were observed in other ferroelectric pyridinium salts $PyBF_4$ [6] and $PyClO_4$ [7], which means that a substitution of different kinds of anion in pyridinium salts results in substantial changes in crystal structures and physical properties of these compounds.

4. Conclusions

(1) $PyIO_4$ was found to undergo a series of structural phase transitions characterized by the following changes of symmetry: $Cmcm \overset{321\ K}{\longrightarrow} Cmc2_1 \overset{210\ K}{\longrightarrow} C2$.
(2) The room temperature and low temperature phases are ferroelectric.
(3) In ferroelectric phases pyridinium cations undergo reorientations among inequivalent energy barriers about an axis perpendicular to the cation plane.
(4) In the paraelectric phase pyridinium cations undergo reorientations among equivalent energy barriers about an axis perpendicular to the cation plane.
(5) The critical slowing down phenomenon was observed at temperatures close to the ferroelectric phase transition, which testifies to the order–disorder character of the phase transition.

(6) The nature of the ferroelectricity of $PyIO_4$ is related to the change of disorder of the pyridinium cations as well as to the appearance of the dipole moment of IO_4^- anions.
(7) $PyIO_4$ belongs to the single-axis class of ferroelectrics.

Acknowledgments

This work was supported by the State Committee for Scientific Research under grant no 2P03B15615.

References

[1] Pająk Z, Czarnecki P, Wąsicki J and Nawrocik W 1998 *J. Chem. Phys.* **109** 6420
[2] Dutkiewicz G and Pająk Z 1998 *Z. Naturf.* b 1998 **53** 1323
[3] Czarnecki P, Nawrocik W, Pająk Z and Wąsicki J 1994 *Phys. Rev.* B **49** 1511
[4] Czarnecki P, Nawrocik W, Pająk Z and Wąsicki J 1994 *J. Phys.: Condens. Matter* **6** 4955
[5] Wąsicki J, Czarnecki P, Pająk Z, Nawrocik W and Szczepański W 1997 *J. Chem. Phys.* **107** 576
[6] Czarnecki P, Katrusiak A, Szafraniak I and Wąsicki J 1998 *Phys. Rev.* B **57** 3326
[7] Czarnecki P, Wąsicki J, Pająk Z, Goc R, Małuszyńska H and Habryło S 1997 *J. Mol. Struct.* **404** 175
[8] Czarnecki P and Małuszyńska H 2000 *J. Phys.: Condens. Matter* **12** 4881
[9] Wąsicki J, Pająk Z and Kozak A 1990 *Z. Naturf.* a 1990 **45** 33
[10] Ripmeester J A 1986 *J. Chem. Phys.* **85** 747
[11] Ito Y, Asaji T, Ikeda R and Nakamura D 1988 *Ber. Bunsenges. Phys. Chem.* **92** 885
[12] Kozak A, Grottel M, Wąsicki J and Pająk Z 1994 *Phys. Status Solidi* a **143** 65
[13] Kozak A, Wąsicki J and Pająk Z 1996 *Phase Transitions* **57** 153
[14] Wąsicki J, Kozak A, Pająk Z, Czarnecki P, Belushkin A V and Adams M 1996 *J. Chem. Phys.* **105** 9470
[15] Ecolivet C, Czarnecki P, Wąsicki J, Beaufils S, Girard A and Bobrowicz-Sarga L 2001 *J. Phys.: Condens. Matter* **13** 6563
[16] Pająk Z, Połomska M and Wolak J 2001 *Solid State Commun.* **119** 137
[17] Czapla Z, Dacko S and Kosturek B 2000 *Z. Naturf.* a **55** 891
[18] Lewicki S, Pająk Z, Porzuckowiak W and Wąsicki J 1995 *Proc. 28th NMR Seminar (Kraków) Report* 171/PL p 190
[19] Sheldrick G 1997 *SHELXS-97 Program for Crystal Structure Determination* University of Gottingen
[20] Sheldrick G 1997 *SHELXL-97 Program for Crystal Structure Determination* University of Gottingen
[21] Flack H D 1983 *Acta Crystallogr.* A **39** 876
[22] Look D C and Lowe I J 1966 *J. Chem. Phys.* **44** 3437
[23] Anderson J E 1973 *J. Magn. Reson.* **11** 398
[24] Lewicki S, Wąsicki J, Czarnecki P, Szafraniak I, Kozak A and Pająk Z 1998 *Mol. Phys.* **94** 973
[25] Blombergen N, Purcell E M and Pound R V 1948 *Phys. Rev.* **73** 679
[26] Polak M and Alion D C 1977 *J. Chem. Phys.* **67** 3029
[27] Wąsicki J, Lewicki S, Czarnecki P, Ecolivet C and Pająk Z 2000 *Mol. Phys.* **98** 643